Residential Heat Pump as Flexible Load for Direct Control Service with Parametrized Duration and Rebound Effect

Emeline Georges[a,*], Bertrand Cornélusse[b], Damien Ernst[b], Vincent Lemort[a], Sébastien Mathieu[b]

[a] *Energy Systems Research Unit, Thermodynamics Laboratory, University of Liège, Liège, Belgium*
[b] *Systems and Modeling Research Unit, Department of Electrical Engineering and Computer Science, University of Liège, Liège, Belgium*

Abstract

This paper addresses the problem of an aggregator controlling residential heat pumps to offer a direct control flexibility service. The service consists of a power modulation, upward or downward, that is activated at a given time period over a fixed number of periods. The service modulation is relative to an optimized baseline that minimizes the energy costs. The load modulation is directly followed by a constrained rebound effect, consisting of a delay time with no deviations from the baseline consumption and a payback time to return to the baseline state. The potential amount of modulation and the constrained rebound effect are computed by solving mixed integer linear problems. Within these problems, the thermal behavior of the building is modeled by an equivalent thermal network made of resistances and lumped capacitances. Simulations are performed for different sets of buildings typical of the Belgian residential building stock and are presented in terms of achievable modulation amplitude, deviations from the baseline and associated costs. A cluster of one hundred ideal buildings, corresponding to retrofitted freestanding houses, is then chosen to investigate the influence of each parameter defined within the service. Results show that with a set of one hundred heat pumps, a load aggregator could expect to harvest mean modulation amplitudes of up to 138kW for an upward modulation and up

*Corresponding author
Email address: emeline.georges@ulg.ac.be (Emeline Georges)

Accepted in *Applied Energy* (DOI:10.1016/j.apenergy.2016.11.012)

to 51kW for a downward modulation. The obtained values strongly depend on the proposed flexibility service. For example, they can decrease down to 2.6kW and 0.4kW, respectively, if no rebound effect is allowed.

Keywords: Heat pumps, Linear programming, Load management, Load modeling, Optimization methods, Power systems

1. Introduction

The increase in decentralized power generation and the integration of intermittent renewable energy sources in electrical distribution systems have entailed a rising interest in the use of load modulation services [1]. These services are provided by load aggregators which manage and trade the demand flexibility of electricity consumers. Among flexible loads, thermostatically controlled loads (TCLs) have been shown to present suitable characteristics for active demand response through the manipulation of temperature set points [2, 3]. Different signals are used to trigger load modulation: forward price signals [4, 5], power flow and voltage level in a distribution line [6] and residual load [7]. Two mainstream approaches are distinguished. The first one takes the point of view of the end-user and aims at maximizing its financial benefit [8, 4, 9, 10]. The second approach is based on a centralized method to meet system-level needs, such as load following [11, 12], minimum electricity generation costs or CO2 emissions [13]. To this end, end-users are pooled to provide an aggregated flexible load [14, 15].

This study takes the point of view of a load aggregator controlling a cluster of domestic heat pumps. The aggregator wants to offer direct control flexibility services. The services consist of an upward or downward modulation for a fixed number of periods followed by a constrained number of periods characterizing the rebound effect. The achievable power modulation amplitude is determined with respect to a reference baseline. This baseline is such that it minimizes the energy costs for the end-user. The activation of the flexibility is performed in three steps: (i) the modulation, (ii) a delay period with no deviations from the baseline consumption, and (iii) a payback period during which deviations in consumption occur to allow the heat pumps to return to their baselines. The amplitudes of the achievable modulations and of the deviations during the payback are well defined within the service.

The interest in quantifying the flexibility of heat pumps within a well-defined flexibility service resides in the opportunity to exchange it as a commodity in the electrical system and electricity markets. Different actors could resort to this flexibility service: an electricity retailer could use it either to balance its portfolio as a balance-responsible party or to adjust its consumption according to day-ahead spot market prices. In the electricity market, deviations from the positions stated to the system operator, in this case, the baselines, expose the market participant to a penalty based on the imbalance tariff. Therefore, the knowledge of the payback following the modulation is key information to activate the flexibility service. A system operator could rely on the service to relieve a congestion in a line or a transformer. The quantification of the payback resulting from the modulation allows the system operator to activate the service without creating congestions further in time. Finally, a system operator could also rely on this service for balancing purposes [16, 17]. Here again, the knowledge of the payback avoids the system operator reaching an unpredicted system imbalance following the activation of the modulation.

The following studies focus on detailed demand-side models with TCLs. Pavlak et al. [18] investigate the potential of using the thermal mass of office buildings to minimize peak demand. A day-ahead multi-objective optimization is implemented to provide the modulation service at minimum cost for the end-user and minimum frequency regulation cost. The optimization also determines the optimal time period to activate the load modulation. The study is extended to a portfolio of office buildings in [19] and the possible additional benefits retrieved from synergies between the buildings are outlined. De Coninck and Helsen [20] propose a bottom-up approach to determine the flexibility of buildings and heating, cooling and air-conditioning systems is developed. Three optimal control problems are solved to determine, first, a cost-optimal baseline for the consumer, and then, the maximum upward and downward modulations available during a given time span of the day. Ali et al. [21] propose a similar optimization scheme to [20] that is applied to residential demand response. The cost-optimal day-ahead prediction of the baseline is followed by an intra-day modulation with the introduction of "bonus" price incentives. A sensitivity study of the percentage of storage capacity allocated to the day-ahead and to the intra-day optimizations is carried out. The study also proposes a method to aggregate cost functions to optimize a cluster of systems and to model the price elasticity of such loads for unit commitment applications.

In light of the literature review, the first contribution of this paper lies in the investigation of a flexibility service with detailed models of thermostatically controlled loads. The second contribution is the characterization of the payback following the activation of the upward and downward power modulation service and of its influence on the achievable modulation amplitude for different periods of the day. The characterization of the payback is particularly useful for operational planning of the distribution network and real-time activation of the service by different actors. The methodology is therefore complementary to the methods presented in [20] and [21] by constraining the payback time and characterizing the rebound effect in terms of costs and energy volumes, and it differs from [18] in which the payback time is a result of the optimization scheme with a unique daily value. In this paper, flexibility can be activated at any moment to tackle unpredicted issues in the electrical system.

The paper is organized as follows. Section 2 defines the flexibility service. Models of the flexible thermal loads are provided in Section 3. Section 4 presents the two optimization problems to solve to obtain the baseline profiles and amplitudes of modulation. Section 5 presents the cluster of buildings representative of the Belgian residential building stock used to illustrate the method. Results are then presented in Section 6. Parametric studies are conducted to highlight the influence of the different parameters that characterize the service. Finally, Section 7 concludes the study.

2. Load modulation service

The mechanism considered in this paper is a flexibility service consisting in the activation of a load modulation in a given period τ and a constrained rebound effect. The modulation service can be activated during n consecutive periods. The activation is directly followed by a delay of l periods before a payback of k periods which compose the rebound effect. Within the delay, there is no deviation from the target consumption. During the payback, deviations in consumption are allowed for the system to return to its predefined state after the k periods. A graphical representation of the service is provided in Fig. 1. The objective of the aggregator is to obtain the maximum modulation amplitude over the n periods, $\delta_\tau, ..., \delta_{\tau+n-1}$, positive for an upward activation and negative for a downward activation, with minimum payback in the k periods. The dead band of l periods between activation and

payback is introduced to mitigate and delay potential additional stresses on the electricity grid brought by the deviations inherent to the payback.

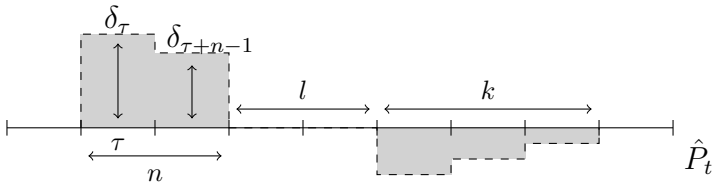

(a) Modulation signal.

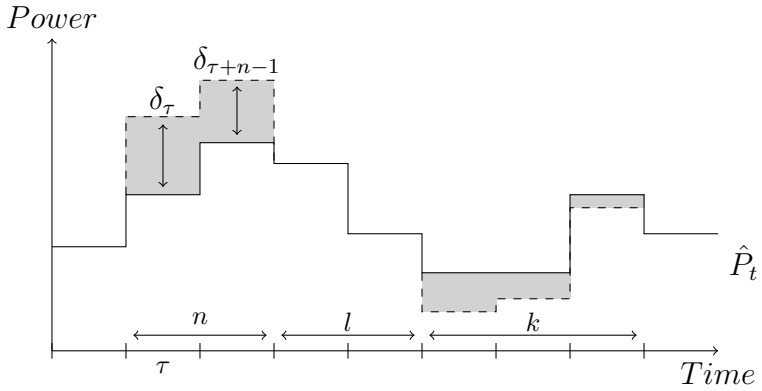

(b) Modulation added to the baseline.

Figure 1: Upward modulation during n periods with a payback of k periods delayed by l periods.

A modulation must be defined with respect to a reference consumption pattern [22]. In this article, we take as reference a baseline $\hat{P}_t$ that minimizes the consumer electricity cost. This choice has two motivations. First, the use of flexible heat pumps should benefit the end-user. Minimizing the energy costs appears to be a good incentive for consumers to enroll in flexibility programs proposed by aggregators. The second motivation lies in the possibility for an aggregator to be a balance responsible party, which compels it to state its positions to the system operator prior to real-time. In this work, these baselines are computed by the aggregator and used as references to quantify the power modulations and resulting deviations.

The proposed flexibility service is the result of the aggregation of a set of houses equipped with heat pumps. A typical case is an electricity retailer using the flexibility of its clients to balance its own portfolio as a balance-

responsible party. Another example is an aggregator proposing its services to a distribution system operator willing to relieve a congestion in a line or a transformer or to a transmission system operator for its secondary reserve. The aggregator proposes the service detailed in this section to another actor. Using flexibility for self-balancing would not require to define a flexibility service but only to directly optimize the consumption. The actual volume activated by the other actor may be less or equal to the total potential. The purpose of the activation is application dependent and is out of the scope of this paper. The service provides all necessary information: the available potential of flexibility and the cost and deviations entailed by the activation of the service. With this information, the other actor is able to make a decision without having to directly manage each individual heat pump.

3. Buildings and heat pumps

The heat demand from the buildings can be determined using models containing different levels of details. Grey-box models are simplified models providing an accurate representation of the thermal response of a building with reduced computational requirements [23]. The building thermal behavior is modeled by an equivalent thermal network consisting of thermal resistances, R in K/W, and lumped thermal capacitances, C in J/K. The RC parameters of the network can either be identified from validated models with higher level of details or imposed by normative definitions, such as in [24]. For the purpose of this study, two different single zone 5R3C models are used. They are illustrated in Fig. 2. The first model structure, referred to as Model I, is a trained model presented in [9], and used to model typical retrofitted freestanding buildings. The second one, referred to as Model II, is a modification of the ISO13790 model [24] by the introduction of two additional lumped thermal capacitances taking into account the non-homogeneous air distribution in the zone and the thermal capacity of the internal walls. It is used for the large-scale application of the proposed method, when lack of available data prevents all buildings from being modeled with identified parameters.

Such models allow a straightforward linear state-space formulation of the governing differential equations as follows

$$\mathbf{x}^s_{t+1} = \mathbf{A}^s\mathbf{x}^s_t + \mathbf{B}^s\mathbf{u}^s_t + \mathbf{E}^s Q^s_t \tag{1}$$

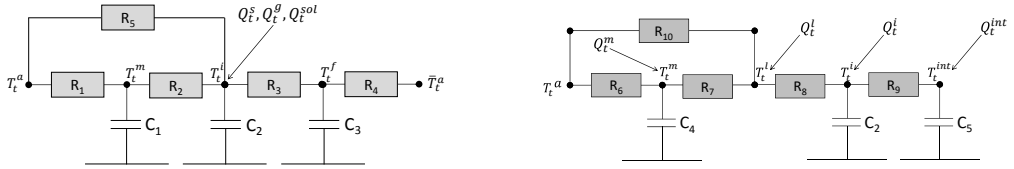

(a) Model I: model trained from detailed building simulation tools.

(b) Model II: model modified from ISO13790 model [24].

Figure 2: 5R3C Grey-box model structures.

where Q_t^s is the space heating thermal power in period t. In Model I, the state vector $\mathbf{x}_{t+1}^s$ is a three-element vector composed of the indoor air temperature, T_t^i, the wall mass temperature, T_t^m, and the floor temperature, T_t^f. In Model II, the state vector $\mathbf{x}_{t+1}^s$ is a three-element vector composed of the indoor air temperature, T_t^i, the massive external walls temperature, T_t^m and the massive internal walls temperature, T_t^{int}. $\mathbf{u}_t^s$ is a four-element vector composed of the uncontrolled model inputs, i.e. the outdoor air temperature, T_t^a, the yearly average outdoor air temperature, $\overline{T}_t^a$, the solar gains, Q_t^{sol} and the internal gains due to occupants and electrical appliances, Q_t^g. In Model II, solar and internal gains are distributed amongst heat gains Q_t^i, Q_t^l, Q_t^m and Q_t^{int} on the different temperature nodes as described in [24]. The matrices $\mathbf{A}^s, \mathbf{B}^s$ and $\mathbf{E}^s$ are equivalent RC parameters of the state space model dependent on the house modeled.

Indoor thermal comfort for the occupants should be satisfied at any time as imposed by the constraint

$$T_t^{min} \leq T_t^i \leq T_t^{max}. \tag{2}$$

The domestic hot water tank is modeled using a one-node capacitance model with homogeneous water temperature $\mathbf{x}_t^w$. Heat losses to the ambiance are considered. The energy conservation law can be expressed by the state-space formulation

$$\mathbf{x}_{t+1}^w = \mathbf{A}^w T_t^w + \mathbf{B}^w \mathbf{u}_t^w + \mathbf{E}^w Q_t^w \tag{3}$$

where Q_t^w is the domestic hot water heating demand in period t and T_t^w is the water temperature in the tank constrained by

$$T^{min} \leq T_t^w \leq T^{max} \tag{4}$$

The input vector $\mathbf{u}_t^w$ is composed of the outdoor air temperature and the mains water temperature. The matrices $\mathbf{A}^w, \mathbf{B}^w$ and $\mathbf{E}^w$ are parameters of the state space model dependent on the house modeled.

Variable-speed air-to-water heat pumps are used to cover the domestic hot water and heating needs of the houses. The choice of variable-speed technology is driven both by the higher efficiency at part-load and by the larger flexibility to perform load following. They are modeled using a linear empirical model based on the ConsoClim method proposed by [25], and presented in Equations (5a) to (5d). The same model is used for space heating and domestic hot water, and it only differs by the temperature of the water supplied to the house and that of the water tank, T^{su} in K. The model determines the parameter $W_t^{\max}$ linked to the coefficient of performance (COP) of the heat pump, which is later used to obtain the relation between electrical power W_t and heat demand Q_t.

$$Q_t^{max} = (d_0 + d_1(T_t^a - T^{a,n}) + d_2(T_t^{su} - T^{su,n}))Q^n \tag{5a}$$

$$\Delta T_t = \frac{T_t^a}{T_t^{su}} - \frac{T^{a,n}}{T^{su,n}} \tag{5b}$$

$$COP_t^{\max} = \frac{COP^n}{c_0 + c_1\Delta T_t + c_2\Delta T_t^2} \tag{5c}$$

$$W_t^{max} = \frac{Q_t^{max}}{COP_t^{max}} \tag{5d}$$

Equation (5a) determines the maximum thermal power that can be supplied by the heat pump for given ambient and water supply temperatures. The coefficient of performance is determined by Equation (5c) and the corresponding electrical consumption of the compressor is given by Equation (5d). The part-load electrical consumption of the variable-speed compressor, W_t is expressed as a function of the part-load heat demand, Q_t, using the following piecewise linear approximation

$$W_t = f_1 \frac{Q_t}{Q_t^{max}} W_t^{max} \qquad for\ \frac{Q_t}{Q_t^{max}} \leq 0.3 \tag{6a}$$

$$W_t = \left(f_2\left(\frac{Q_t}{Q_t^{max}} - 0.3\right) + f_3\right) W_t^{max} \qquad for\ 0.3 < \frac{Q_t}{Q_t^{max}} \leq 1 \tag{6b}$$

The parameters of the heat pump model, a_i, b_i and f_i, used in Equations (5) and (6) are calibrated based on manufacturer data. Technical constraints

prevent the heat pump from working simultaneously to supply heat to the domestic hot water tank and to the space heating system. To prevent the damage of mechanical components, decisions to start or stop the heat pump should not occur more than eight times an hour. This precaution is ensured by a decision time step of 15 minutes.

4. Optimization problems

This section presents the two optimal control problems which an aggregator solves in order to propose flexibility services. The first problem is to determine the electrical consumption of each building that minimizes energy costs in response to a forward retail price signal. This consumption profile, referred to as baseline consumption, is then used as an input for the second optimization problem. The latter determines the maximum upward or downward modulation amplitude that can be achieved from the baseline profile in a given time period.

In the following subsections, the thermal states transition model and the state constraints defined in Section 3 are summarized by

$$\mathbf{x}_{t+1} = f(\mathbf{x}_t, W_t^s, W_t^w, \mathbf{u}_t) \tag{7a}$$

$$\mathbf{x}_t^{min} \leq \mathbf{x}_t \leq \mathbf{x}_t^{max} \tag{7b}$$

where $\mathbf{x}_t$ is the vector of the state variables, and W_t^s and W_t^w are the optimization variables corresponding to the heat pump consumption for space heating and for domestic hot water heating, respectively. $\mathbf{u}_t$ represents the set of time-dependent input parameters of the building model.

4.1. Baseline electricity consumption profile

The first optimization problem is solved in order to obtain a base consumption profile that minimizes the energy costs of the heat pump's owner. This baseline is denoted by $\hat{P}_t$ and the corresponding states are denoted by $\hat{\mathbf{x}}_t$. This optimization problem is written as

$$\min \sum_{t \in \mathcal{H}} \left(\pi_t^+ P_t^+ - \pi_t^- P_t^- \right) dt \tag{8a}$$

subject to,

$$\hat{P}_t = P_t^+ - P_t^- \qquad \forall t \in \mathcal{H} \tag{8b}$$
$$\hat{P}_t = \hat{W}_t^s + \hat{W}_t^w + \Gamma_t \qquad \forall t \in \mathcal{H} \tag{8c}$$
$$\hat{\mathbf{x}}_{t+1} = f(\hat{\mathbf{x}}_t, \hat{W}_t^s, \hat{W}_t^w, \mathbf{u_t}) \qquad \forall t \in \mathcal{H} \tag{8d}$$
$$\mathbf{x}_t^{min} \leq \hat{\mathbf{x}}_t \leq \mathbf{x}_t^{max} \qquad \forall t \in \mathcal{H} \tag{8e}$$
$$0 \leq \hat{W}_t^s \leq \hat{y}_t W_t^{s,max} \qquad \forall t \in \mathcal{H} \tag{8f}$$
$$0 \leq \hat{W}_t^w \leq (1 - \hat{y}_t) W_t^{w,max} \qquad \forall t \in \mathcal{H} \tag{8g}$$
$$P_t^-, P_t^+ \geq 0 \qquad \forall t \in \mathcal{H} \tag{8h}$$
$$\hat{y}_t \in \{0, 1\} \qquad \forall t \in \mathcal{H} \tag{8i}$$

The duration of a period is given by dt, which for one quarter equals 0.25 h. $\mathcal{H}$ is the optimization horizon composed of H periods. The amount of power bought from or sold to the grid in period t, P_t^+ and P_t^-, respectively at the prices π_t^+ and π_t^- in €/kWh, is given in Equation (8b). It is defined in Equation (8c) by the sum of the heat pump consumption for space heating, $\hat{W}_t^s$, or domestic hot water heating, $\hat{W}_t^w$, and of the exogenous consumption, Γ_t, corresponding to the net power consumed by other electric appliances or produced by decentralized electricity generation units. We assume $\pi_t^+ > \pi_t^-$. The case of an equality can be handled by removing constraint (8b) and using $\hat{P}_t$ in the objective function. The fact that heat pumps cannot be used simultaneously for space heating and domestic hot water heating is modeled by a binary variable $\hat{y}_t$, which is equal to one if the heat pump is used for space heating and equal to zero for domestic hot water production.

4.2. Achievable modulation amplitude

The baseline consumption, $\hat{P}_t$, is given as input to a second optimization problem. The objective of the latter is to obtain the maximum upward modulation in a period τ over n consecutive periods, with a payback effect over k periods and delayed from the modulation by l periods. The maximum modulation available in one house at a given period τ over n periods is denoted by δ_τ^*. In the case of an upward modulation, the corresponding optimization problem is written as:

$$\max \delta_\tau^* - \epsilon I^+ - \epsilon I^- \tag{9a}$$

subject to, $\forall t \in \mathcal{K}(\tau, n+l+k-1)$:

$$P_t = W_t^s + W_t^w + \Gamma_t \tag{9b}$$
$$P_t = \hat{P}_t + \delta_t \tag{9c}$$
$$0 \leq W_t^s \leq y_t W_t^{s,max} \tag{9d}$$
$$0 \leq W_t^w \leq (1-y_t) W_t^{w,max} \tag{9e}$$
$$\mathbf{x}_{t+1} = f(\mathbf{x}_t, W_t^s, W_t^w, \mathbf{u_t}) \tag{9f}$$
$$\mathbf{x}_t^{min} - \lambda \leq \mathbf{x}_t \leq \mathbf{x}_t^{max} + \lambda \tag{9g}$$

and,

$$\mathbf{x}_\tau = \hat{\mathbf{x}}_\tau \tag{9h}$$
$$\forall t \in \mathcal{K}(\tau, n-1) : \delta_t \geq \delta_\tau^* \tag{9i}$$
$$\forall t \in \mathcal{K}(\tau+n-1, l) : \delta_t = 0 \tag{9j}$$
$$\forall t \in \mathcal{K}(\tau+n+l-1, k) : -I^- \leq \delta_t \leq I^+ \tag{9k}$$
$$-\sigma \leq \hat{\mathbf{x}}_{\tau+n+l+k} - \mathbf{x}_{\tau+n+l+k} \leq \sigma \tag{9l}$$

$\mathcal{K}$ is the flexibility service horizon, composed of n periods of modulation followed by $l+k$ rebound periods. Equation (9c) defines the modulation that can be achieved with respect to the baseline. In constraint (9g), the parameter λ is used to relax the state constraint (8e) to improve the modulation potential. The initial condition of the state is given by equation (9h). Constraint (9i) expresses that the modulation amplitudes over the n consecutive periods should be greater than a common minimum value. Equality (9j) delays the payback effect by l periods after the modulation period. Variables I^+ and I^- are the maximum positive and negative deviations with respect to the baseline on the payback horizon. These deviations are penalized by a parameter ϵ set to 0.5. This choice is motivated in Section 6. Finally, equality (9l) ensures that the state at the end of the payback horizon is close enough to the one given by the baseline. Since the state transition only depends on the previous state and the power consumed by the heat pump, this condition ensures that there are no major deviations from the baseline after the payback horizon. The case of maximum downward modulation is obtained by replacing (9a) by $\min \delta_\tau^* + \epsilon I^+ + \epsilon I^-$ and (9i) by $\delta_t \leq \delta_\tau^* \ \forall t \in \mathcal{K}(\tau, n-1)$.

In the proposed approach, the two optimization problems are solved consecutively, and the determination of the baseline profile is independent of the

modulation. This choice is motivated by the opportunity to use such flexibility service for real-time applications when the baseline consumptions have already been stated on the day-ahead. One could carry out a combined optimization problem which would shape the baseline profile in order to obtain the maximum modulation amplitude in a given time period while minimizing the energy costs.

5. Generation of the test cases

The method is applied to a cluster of buildings representative of the Belgian residential building stock. The characterization of the representative residential buildings in terms of geometry and envelope characteristics comes from study [26]. This study proposes a description of typical Belgian residential buildings with four building configurations, five construction time periods and various insulation levels of the envelope. Geometrical and building envelope data are available in an *Excel* document and are straightforward to couple to building simulation and optimization tools. The four building configurations are freestanding, semi-detached and terraced houses, and apartments. Apartments in large buildings are often equipped with centralized heating production plants supplying all of them. The flexibility service therefore depends on a cluster of aggregated customers, for which the proposed method cannot be applied directly. For this reason, in the present work, only freestanding, semi-detached and terraced houses are considered. Among the representative buildings, 41% present sufficient envelope insulation levels to be potentially equipped with residential air-to-water heat pumps to supply both heating and domestic hot water needs. The selection criterion requires the maximum heating load of the building to be less than the largest residential single-stage heat pump capacity available on the market. For this set of buildings, the average heat pump nominal electrical power is 4.6 kW. Nominal conditions are defined based on those in [27] for a 7°C outdoor temperature and a water temperature adapted to the house insulation level. Additional resistances of 3 to 5kW, depending on the house insulation level, are used as backups to cover the heat demand for space heating during the coldest days of the year.

The number of inhabitants in each house is drawn from a normal distribution of an average of three and a standard deviation of two with a maximum of five occupants. The exogenous consumption profiles associated with lighting and appliances are obtained from article [28], as well as the domestic

hot water draw-off events. Indoor temperature set point schedules are intermittent temperature profiles generated based on normal distribution laws for morning, midday and evening start-up times. All profiles have a weekly average indoor set point above 18°C. Occupancy profiles are derived from the latter. Indoor thermal comfort for occupants should be satisfied at all times. During the heating season, the indoor air temperature is constrained to deviate a maximum of 1°C from the imposed set point during occupied periods of the daytime, and within 1°C of the extreme limits of the daily set point during unoccupied periods. In the summer, the lower limit of the indoor air temperature is set to 1°C below the imposed set point. The upper limit can vary, since no cooling system is considered.

Buildings are equipped with conventional hydronic radiators. The temperature of the water supplied to the radiator is adjusted according to the insulation level of each building. The radiators are assumed to be sized so that they are able to supply the thermal power required by the building at any time and the dependency of the emitted heat on the water supply temperature is not modeled. The domestic hot water tank lower limit in Equation (4) is imposed by sanitary constraints to 50°C, whereas the upper limit of 65°C is imposed by the heat pumps design. The tank volume is adapted for each house based on a water consumption of 50 liters per person per day, along with an additional safety volume of 50 liters. It is therefore comprised between 100 and 300 liters. The supply temperature is set to 65°C in Equations (5a) and (5b), which underestimates the performance of the heat pump.

Ten percent of the buildings are also equipped with south or west-oriented PV panels with thirty-five degrees tilt angles and 18% average efficiency. The installed surface area is drawn from a discrete uniform distribution over an interval ranging from ten to thirty-five square meters.

6. Results

The test cases presented in Section 5 are simulated for three and a half days with a time step of fifteen minutes. The optimization results for the first two days serve the purpose of initializing the state variables and are discarded in the following analysis. The extra half day of simulation is used to avoid imposing terminal constraints on the states. The following results therefore focus on the third simulation day. The total modulation potential of an aggregated set of houses is the sum of the potential available for each

house. A set of one hundred buildings offering the most cost-effective service is selected. These buildings are then used to perform parametric studies aiming to identify the influence on the modulation potential of each parameter defined within the service.

The optimization problem is a convex mixed integer linear programming problem (MILP) solved with the open-source MATLAB compatible toolbox YALMIP [29] coupled to CPLEX solver [30]. With a dual core i7 3GHz computer with 16GB RAM, the computation time for a baseline of one day for a single house takes a few seconds. It takes a few milliseconds to compute one modulation in one house in one time period τ with one set of modulation parameters n, l and k. Therefore, if an aggregator has a set of one hundred buildings, the computation of one hundred baselines takes about 8 minutes. For the given modulation parameters, calculating the available upward and downward modulations for the 96 periods of a day for all houses takes about 14 minutes.

6.1. Illustration on a single house

The proposed service is first illustrated in Fig. 3 for a single house representative of houses built between 1991 and 2006 in Belgium. An upward modulation is activated at period 24 for a single period. Delay and pay-back times are set to two and four periods respectively. Figure 3a shows an upward modulation amplitude of about 2.5kW from the baseline. As imposed by the delay parameter l, no deviation occurs during the next two periods. The amplitude of the following payback deviations are comprised within 1.5kW. Figure 3b presents the repartition of the heat pump modulation between space heating mode and domestic hot water mode. The corresponding evolution of the zone and tank temperatures is shown in Fig. 4. The upward modulation in period 24 is carried out by increasing the heat pump power in space heating mode, causing the zone temperature to rise by about 0.5 °C. This entails a reduction in heat demand for space heating at period 25. To ensure no deviation from the baseline consumption over two periods following the modulation, the heat pump switches from space heating to domestic hot water mode. The water temperature increases by about 2°C, as illustrated in Fig. 4b. A payback, contained within four periods, is observed from period 27 to 30. At period 31, both zone and tank temperatures have returned to their baseline level. It should be noted that the large temperature dead band illustrated in Fig. 4a is due to a reduction of temperature set point from 21°C to 18°C overnight.

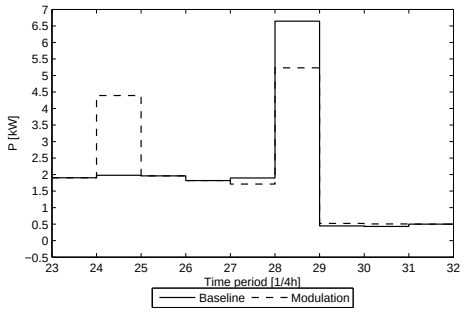

(a) Total power modulation.

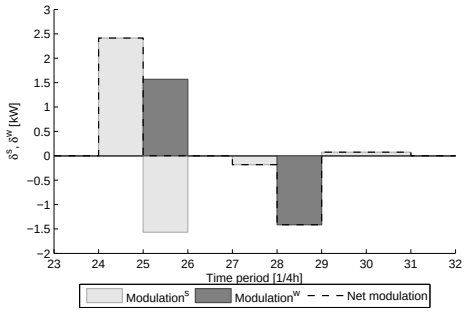

(b) Space heating and domestic hot water power modulation.

Figure 3: Power modulation of a freestanding house built between 1991 and 2006 for an activation in period 24, a delay of two periods and a payback on four periods.

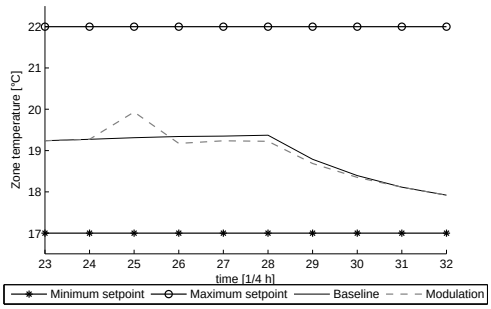

(a) Zone temperature.

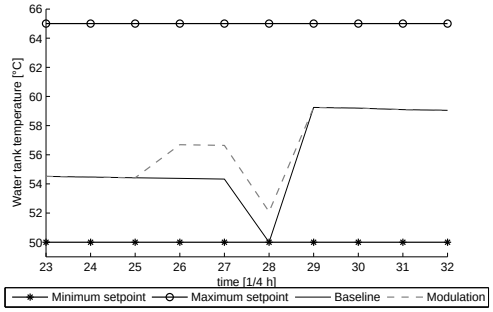

(b) Tank temperature.

Figure 4: Evolution of zone and water tank temperatures during an unoccupied period corresponding to an activation in period 24, a delay of two periods and a payback on four periods, for a freestanding house built between 1991 and 2006.

Heat pump power modulation in heating mode directly affects the thermal comfort of the occupants by deviating from the assumed comfortable baseline. ASHRAE standard 55 defines acceptable indoor air temperature variation rates that respect occupants'comfort [31]. The temperature variation should not exceed 2.2K during one hour period, and 1.1K during any quarter within that one hour period. Figure 5 shows the duration curve of temperature variations for upward and downward activations for the same building for a winter day. The temperature difference between the baseline profile and the modulation is represented by the curve labeled $|\hat{T}_t - T_t|$. The temperature difference between two consecutive time steps of the modulation profile is

denoted $|T_t - T_{t-1}|$. The temperature variation within one hour period for the modulation profile is labeled $|T_t - T_{t-4}|$. This variation is always inferior to 2K. The temperature difference between two consecutive quarters and between the modulation and the baseline always remain inferior to 1.1K. The comfort requirements imposed by the standard are therefore satisfied.

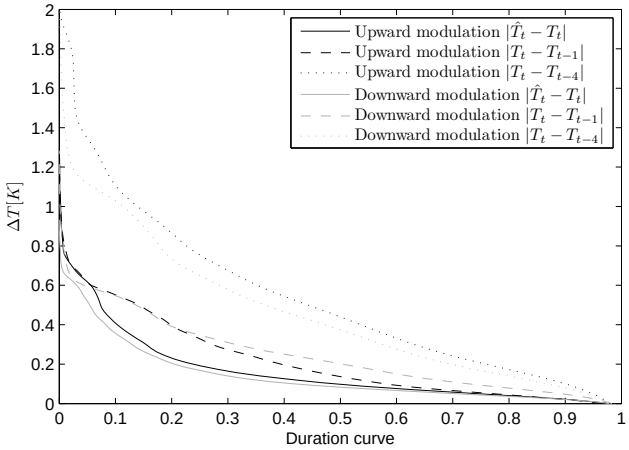

Figure 5: Cumulative frequency density function of temperature differences between baseline and profile after activation and between two successive time steps of the modulation.

6.2. Choice of aggregated set of houses

In this section, the methodology is applied to all types of houses of the Belgian residential building stock that could potentially be equipped with heat pumps. Except for retrofitted freestanding houses built after 1971 for which detailed models are available, all other representative houses are simulated using Model II, as explained in Section 3. For those simulations, the modulation parameters are arbitrarily set to $n = 1$, $l = 0$ and $k = 5$.

In a first simulation set, each house, which represents a share of the building stock, is simulated once. Results are presented in Table 1 and expressed in terms of modulation amplitude and cost per activated volume per house. The cost is obtained by summing the deviations in consumption from the baseline entailed by the activation of the service, and is calculated with the imbalance tariff provided by the transmission system operator [32]. In oder to obtain results per average house, the values obtained for each typical house are multiplied by its representative percentage in the building stock, and then summed. Based on the same weighting average technique, a

distinction can be made between an average house, an average freestanding house, an average semi-detached house and an average terraced house. As seen in Table 1, the upward modulation potential reaches 2.9 kW per house and the downward modulation potential is 0.29 kW per house. The average cost is close to the average Belgian retail electricity tariff for an upward activation and more than double the retail tariff for a downward activation. Terraced houses present a higher potential than the average house for upward modulation, but a reduced downward modulation potential. Freestanding houses offer the highest downward modulation potential. Among freestanding houses built after 1971, some have undergone different levels of retrofitting to improve the insulation of their envelope, and others have been built to meet the legal insulation requirements [33]. Such freestanding houses are represented by four typical building typologies based on the construction time-period, i.e., 1971-1990, 1991-2006 or after 2007, and based on the insulation level, i.e., heavy retrofit (HR) and light retrofit (LR). They are referred to as retrofitted freestanding houses in the remainder of the paper. To further illustrate the proposed method, and to introduce statistical distribution in terms of heat and hot water demand profiles, a second set of simulations focuses on the retrofitted freestanding houses only. To that end, a distribution of the four typical typologies of retrofitted freestanding houses is performed over one hundred houses, proportionally to their share in the building stock. Due to their higher insulation level, retrofitted freestanding houses present a limited upward modulation potential, but the largest downward modulation potential. For both modulations, the activation is the most economical for such houses, as insulation reduces overconsumption. For this reason,the parametric studies carried out in the remainder of the paper focus only on this set of one hundred retrofitted freestanding houses. Their aggregated baseline consumption obtained for a day-night electricity tariff structure is illustrated in Fig. 6 for a winter day, along with the corresponding outdoor temperature. The electricity demand profiles strongly depend on the ambient temperature, but also on the electricity retail tariff. The latter explains the peaks in consumption observed at around 7am, right before the transition to the day-time tariff. The consumption is 53.9 kWh per average house.

Table 1: Modulation amplitude and activation cost per house.

Type of buildings	Mean modulation [kW] Up	Down	Cost [€/kWh] Up	Down
Average house - all types	2.90	0.29	0.27	0.69
Average Freestanding	2.10	0.42	0.27	0.70
Average Semi-detached	2.72	0.29	0.27	0.69
Average Terraced	3.95	0.14	0.26	0.57
Retrofitted freestanding	1.07	0.44	0.19	0.27

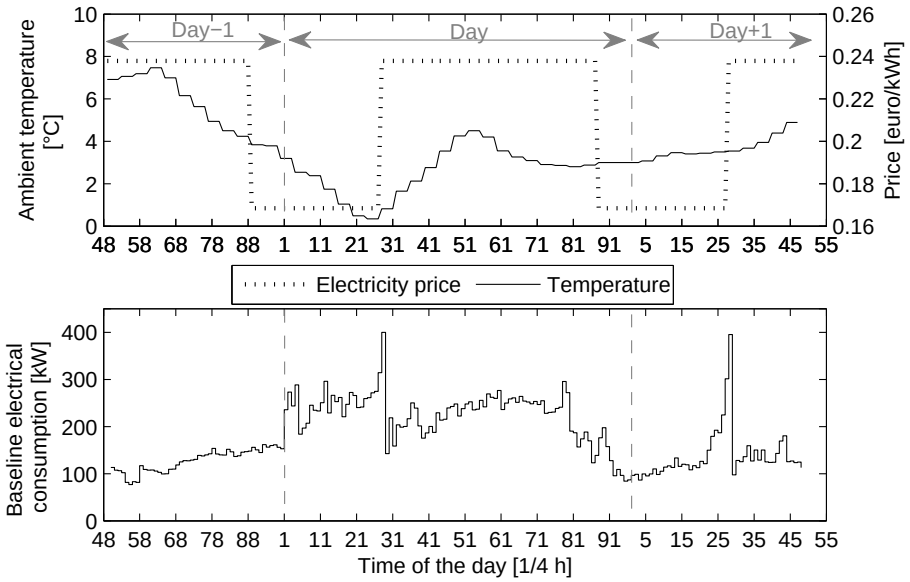

Figure 6: Optimal baseline electricity consumption of one hundred retrofitted freestanding houses on January 24th and corresponding ambient temperature profile and electricity retail price profile.

6.3. Impact of power deviation amplitude limitation

The cost function presented in Equation 9a is parametrized using the payback weight parameter ϵ. This parameter weighs the relative importance of the payback deviations compared to the modulation amplitude in the objective function (9a). For example, Fig. 7 illustrates the impact of this parameter on the maximum modulation amplitude and the amplitude of the deviations for the four types of representative houses investigated and for an

activation in period 18. Modulation service parameters n, l and k are set to one, zero and five periods respectively. For the four houses, as ϵ increases, the maximum modulation amplitude decreases. Houses built between 1971 and 1990 are the most impacted, particularly for downward activations. Indeed, the downward activation potential reaches zero for values of ϵ greater than 0.43 for lightly renovated houses and greater than 0.53 for heavily renovated houses. The upward activation potential tends towards zero for values of 0.7 and 0.88, respectively. In the case of a downward activation, the reduction in achievable modulation amplitude with ϵ is explained as follows. The decrease in heat pump power consumption at a given time τ is usually followed by an increase in consumption during the payback time to return to the baseline. This increase in required power brings the heat pump closer to its full load operating conditions, which are characterized by a lower coefficient of performance for variable-frequency heat pumps. This therefore increases the amplitude of the deviations and is particularly marked for poorly insulated houses, for which the temperature in the zone drops quickly. An inverse trend is observed for upward activations. The increase in power consumption reduces the required power during the payback, which, for the same outdoor conditions, improves the system performance and reduces deviations. The fact that the influence of ϵ on the achievable modulation is stronger for downward modulations than for upward modulations comes from the chosen cost-optimal baseline. The minimization of energy costs tends to drive the temperature trajectory toward the low temperature set points during low price periods, reducing the downward activation potential, but increasing the flexibility for upward activations. For houses built after 1991, the better insulation of the envelope allows to switch the heat pump from heating mode to domestic hot water mode without compromising the occupants' comfort. This mode switch helps reduce the amplitude of the deviations and the influence of ϵ.

In the frame of the modulation service presented in this study, the most suitable service is obtained for a ratio of the modulation amplitude to the maximum deviation amplitude greater than one, i.e.

$$\frac{1}{96}\sum_{\tau=1}^{96}\frac{\sum_{i=1}^{100}\delta_i|_\tau}{\max\left(\sum_{i=1}^{100}I_i^+|_\tau,\sum_{i=1}^{100}I_i^-|_\tau\right)}>1 \tag{10}$$

This ratio increases with ϵ, as illustrated in Fig. 8b for the aggregated set of one hundred houses. However, the number of possible activations, repre-

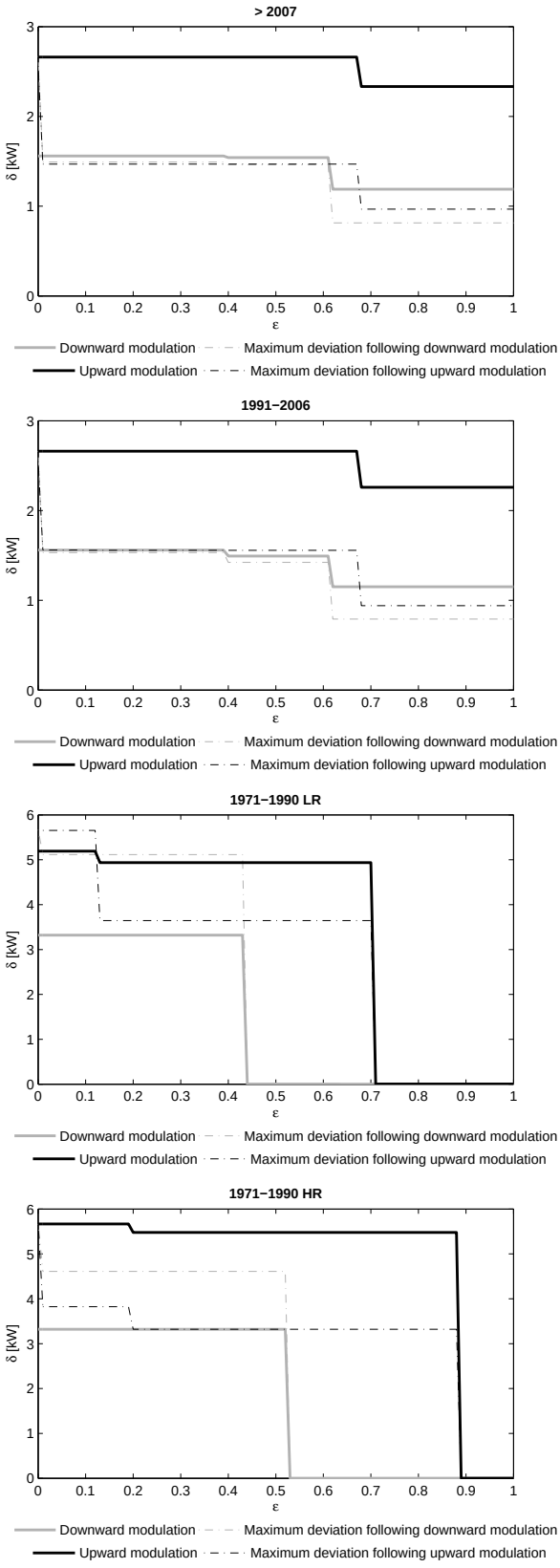

Figure 7: Influence of ϵ on modulation amplitude and related deviations during payback, for $\tau = 18$, $n = 1$, $l = 0$ and $k = 5$.

sented by the mean modulation amplitude per house, decreases when increasing ϵ as shown in Fig. 8a. Therefore, an empirical choice for ϵ corresponds to the value that maximizes the ratio of modulation to deviation (Equation (10)) while limiting the reduction in modulation amplitude. For downward modulations, the optimum is obtained for a value of ϵ equal to 0.52. For upward modulations, the optimum value is located around 0.55. One could also choose an empirical value for each type of house.

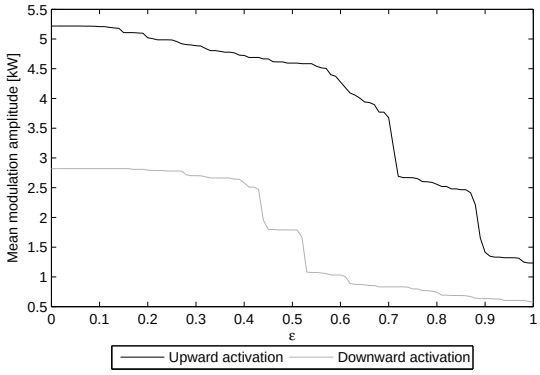

(a) Mean modulation amplitude per house.

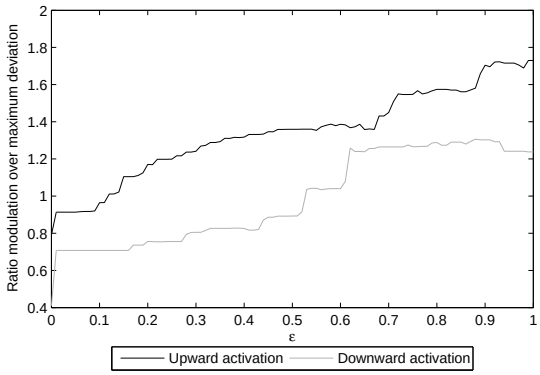

(b) Ratio of the modulation amplitude to the maximum deviation amplitude.

Figure 8: Empirical choice of ϵ based on the maximization of the ratio of the modulation amplitude to the maximum deviations (Equation (10)).

6.4. Time constants of the modulation service

6.4.1. Payback length k

The maximum upward and downward modulations for the aggregated portfolio of one hundred freestanding houses are illustrated in Fig. 9 for a winter weekday and three payback horizon lengths. The largest upward and

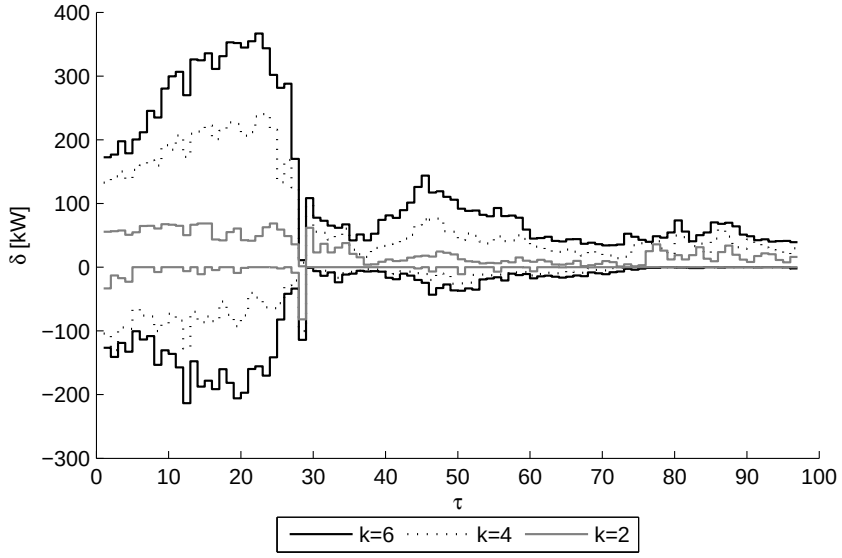

Figure 9: Influence of the payback length on the modulation amplitude for each potential activation period on January 24th for 100 houses.

downward modulations are obtained in periods 0 to 28, with maximum amplitudes reaching 370kW and 210kW, respectively. During that time frame, most of the flexibility is provided by space heating consumption. The temperature profiles present a night setback where the set point is reduced and the allowed temperature range is wider. In addition, the modulation potential tends to follow the outdoor temperature profile. For the upward modulation, there is a maximum in periods 16 to 28. This phenomenon is due to the higher room temperature set point for the daytime, which allows a faster return to the baseline electricity demand of the house. In the case of downward modulation, the limitation of the heat pump capacity reduces the achievable downward modulation as one gets closer to the set point transition. The upward peaks observed in periods 30 and 88 correspond to the start-up of heat pumps to produce domestic hot water after usual morning and evening water draw-off events. During the day, most of the upward and downward modulations are provided by space heating. Flexibility from the

domestic hot water tank is mostly restricted by the high inertia of the water tanks, due to their good insulation. In addition to this inertia, major hot water draw-off events mainly happen in the morning and evening, which limits consumption needs. Within a day, the heat pump is mostly used for space heating, since the deadband of the room temperature is set to only 2°C. Consequently, and with the heat pump being limited to working in one mode at a time, consumption for domestic hot water is mostly concentrated in single periods to give more freedom for space heating. The potential of downward modulation gets close to zero for time periods between 88 and 95. This is explained by the fact that the optimization of the baseline drives the system toward minimizing the costs, and therefore, the temperatures hit their lower bound when the electricity tariff is high. In period 88, the night-tariff starts, but, due to the foreseen night temperature setback, the heat pump is slowed down, therefore reducing the downward modulation potential.

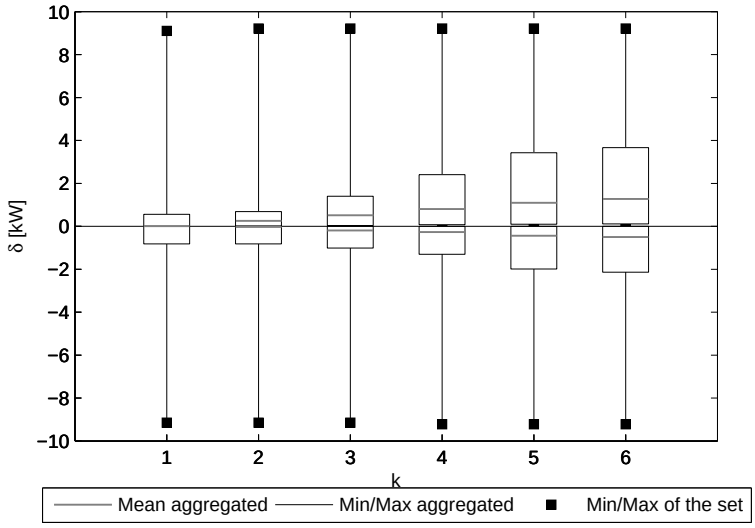

Figure 10: Evolution of the minimum, maximum and mean modulation potentials per average house for the aggregated set of houses, and of the minimum and maximum modulation amplitudes among the set of houses with the payback length.

Figure 10 shows the impact of the payback length on the mean, minimum and maximum achievable modulation per average house. The mean upward and downward modulation amplitudes range from 0.05 to 1.24 kW and from 0.01 to 0.5 kW respectively for payback lengths of one to six periods. The average maximum modulation amplitude of the aggregated set is 3.8 and 1.9

kW respectively, whereas the maximum potential among the set reaches 9kW. For both upward and downward modulations, little improvement is observed in terms of mean and maximum modulation amplitudes when increasing the payback length from 5 periods to 6 periods. A payback duration of one hour and 15 minutes is thus chosen for the rest of the study.

Figure 11 illustrates the seasonal modification of the flexibility potential on the 24th of January, April, June and November. The difference in modulation observed between November and January lies in the higher outdoor temperature, which, combined to the nighttime setback, reduces the flexibility potential for space heating for time periods before period 20. The relative share of electricity consumption devoted to domestic hot water production increases in warmer seasons.

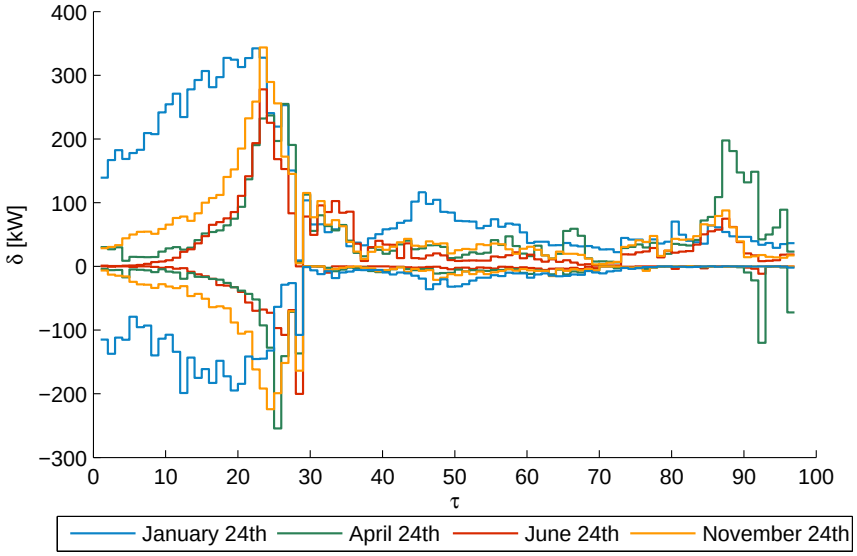

Figure 11: Seasonal influence on the modulation for each activation period on January 24th for 100 houses.

6.4.2. Delay length l

The maximum upward and downward modulations for the aggregated portfolio of one hundred freestanding houses are illustrated in Fig. 12 for a winter weekday, four delay lengths and a payback length of five periods. For all l, the largest upward and downward modulations are obtained in periods 0 to 28, as explained in Section 6.4.1. As l increases from zero to one, a drastic reduction of the downward modulation potential is observed

throughout the day, but most significantly for periods between 10 and 28. For upward activations, a decrease in potential is also observed during that time frame, but is not as strong. The decrease is due to the bounds on the water and indoor air temperatures and to the parametrized objective function, which limits the deviations. Indeed, if at the end of the modulation period, the temperatures have reached their upper or lower bounds, then preventing the heat pump from deviating from its baseline consumption during the next l periods may cause the system to cross the set point limits. Such situations are avoided by reducing the modulation potential and is particularly marked for time periods close to a set point transition, such as in periods 27 to 30.

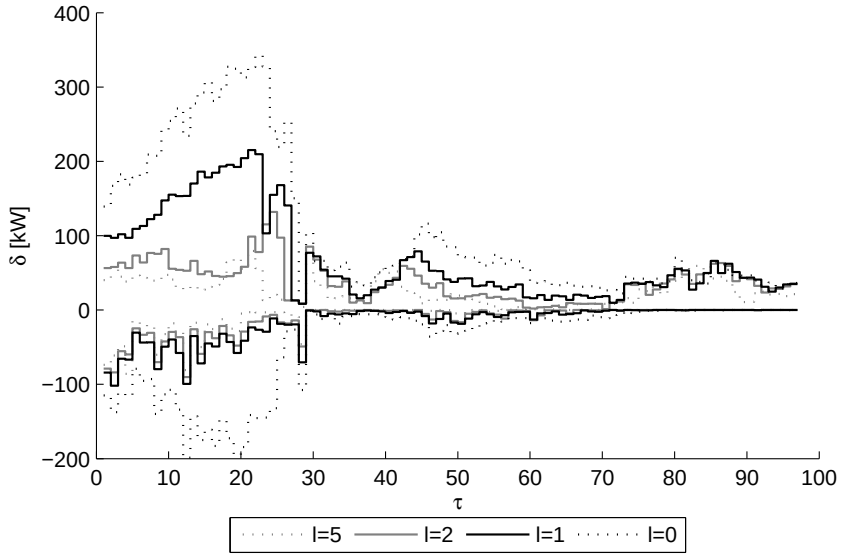

Figure 12: Influence of the delay length before payback on the modulation amplitude for each potential activation period and a payback effect on five periods in January 24th for 100 houses.

The achievable upward modulation amplitude is further reduced when l increases from one to two. For this value, the average activation potentials for the set of houses decrease by 65% and 72% per house, respectively, for upward and downward modulations, as compared to no delay length. Beyond that value, the additional limitations of activation potential entailed by increased values of l are limited, as shown in Fig. 13. Depending on the combination of flexibility service parameters l (0 to 8) and k (1 to 7), the mean upward modulation amplitude varies from 2.6 to 138 kW and the mean downward

modulation amplitude from 0.4 to 51.4 kW for the aggregated set of houses.

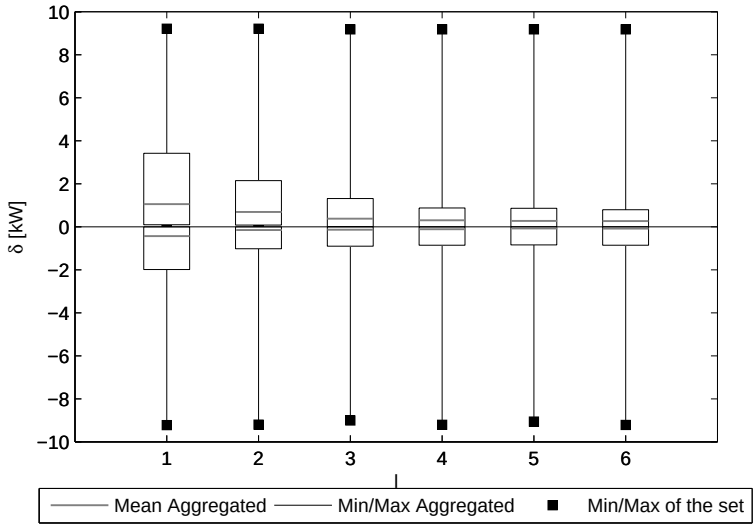

Figure 13: Evolution of the minimum, maximum and mean modulation potentials per average house for the aggregated set of houses and minimum and maximum modulation amplitudes in the set of houses with the delay length l, for a payback over five periods.

6.4.3. Modulation length n

The modulation potential achievable for any time period τ and three different modulation lengths is illustrated in Fig. 14 for one hundred houses on a winter day. Payback and delay lengths are set to five and zero, respectively. As the modulation length increases from fifteen minutes to thirty minutes, the amplitude of activation drops significantly for all periods of the day.

For a modulation length greater than fifteen minutes, a larger modulation potential can be obtained by activating only a subset of heat pumps during each period of the modulation length n. Each group of heat pumps is activated in order to maximize the modulation amplitude in one of the n periods. This is referred to as asynchronous activation and is illustrated in Fig. 15 for a delay length of thirty minutes. Compared to a synchronous activation of the whole set of heat pumps in each of the two periods, the activation of a subset of heat pumps on each period allows for an increase of the minimum upward activation amplitude by up to 110%. However, there exist time periods of the day where it remains more efficient to activate all heat pumps simultaneously during two consecutive periods, such as in period

31 for example. Figure 16 illustrates the number of heat pumps composing each activated subset for a desynchronized upward modulation.

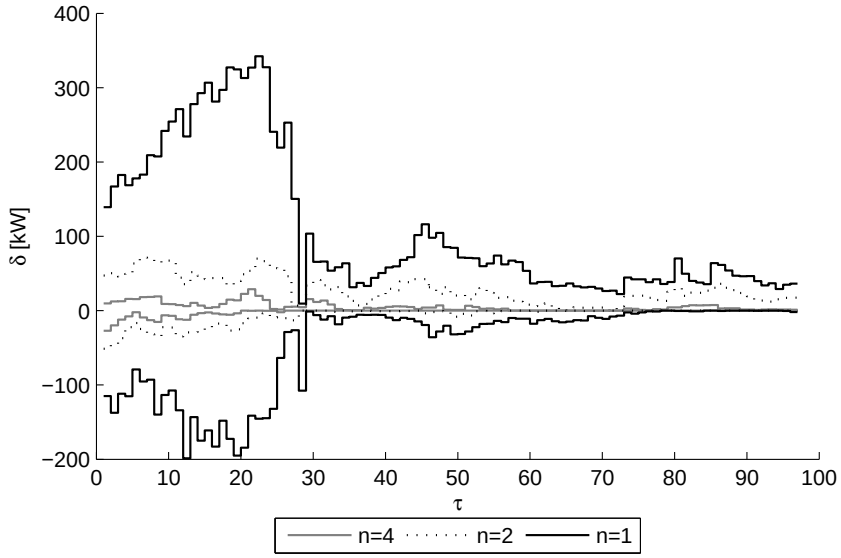

Figure 14: Influence of the modulation length on the average modulation amplitude for each potential activation period in January 24th for 100 houses. Other modulation parameters are set to $l = 0$ and $k = 5$.

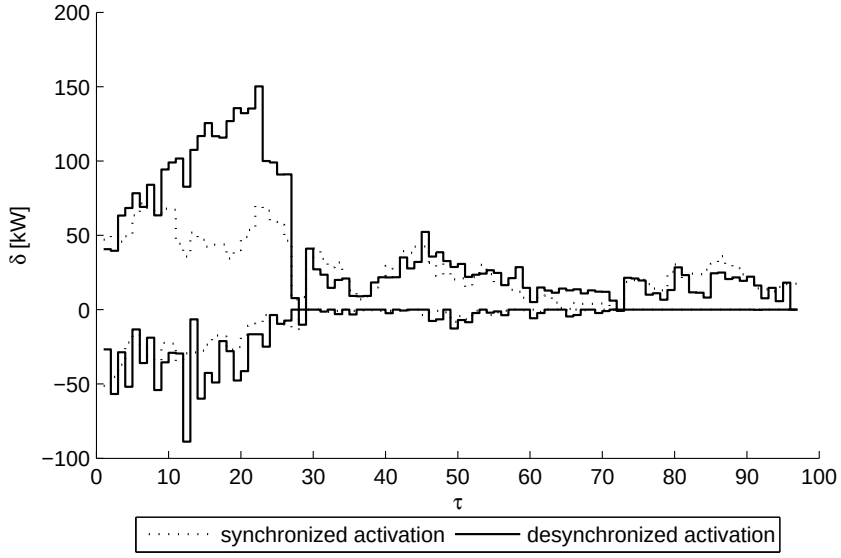

Figure 15: Aggregated modulation amplitude for $n = 2$ for synchronous and asynchronous activations of heat pumps.

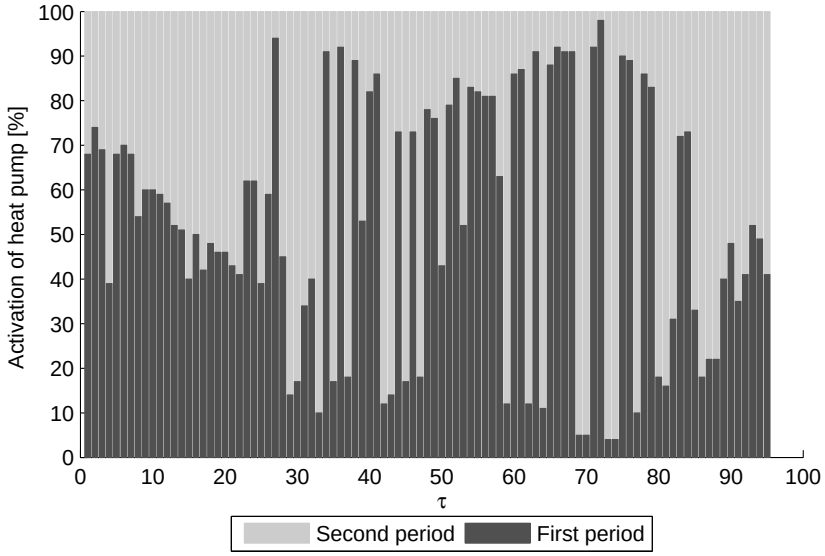

Figure 16: Number of heat pumps activated in each of the two periods for asynchronous upward activations.

6.5. Deviations and overconsumption

Deviations in consumption from the specified baseline are traded on the imbalance market. In the frame of the flexibility service, it is useful to characterize them in duration, amplitude and associated costs.

The volume of deviation is the sum of the absolute differences, during the payback periods, between the baseline consumption and the consumption after modulation. It is interesting to compare it to the energy volume activated by the modulation. For a given delay length, increasing the payback length increases both the achievable modulation amplitude and the relative proportion of deviations. An opposite trend is observed when increasing the delay length for a fixed payback. Depending on the delay and payback lengths, the ratios of deviation over activated volume range from 39% to 123% for upward activations and from 27% to 123% for downward activations.

The activation of a modulation implies an overconsumption, defined as the net difference in energy consumed between the baseline consumption and the consumption with the modulation. The only exception lies in the case of a downward activation with a payback of one period, for which the total energy consumed is smaller than for the baseline. Similarly to the volume of deviation, the overconsumption can be expressed as a percentage of the energy volume activated by the modulation, and ranges from -4% to 83%.

For a fixed delay length, overconsumption increases with the payback time. For each fixed payback time, there exists an optimum delay length that minimizes the ratio of overconsumption to activated volume.

6.6. Influence of the tariff structure

Currently, in Belgium, residential customers can sign up for two types of tariff structures: flat and day/night retail tariffs. In the above sections, the retail tariff used to determine the cost-optimal baseline was the day/night structure. Tariff structures are expected to evolve toward dynamic pricing that reflects the availability of electricity in the market. Such tariffs present variable profiles that have been shown as suitable for demand response programs with heat pumps [9]. An example of a dynamic tariff is illustrated, along with flat and day/night tariffs, in Fig. 17a. The cost of the optimized baseline consumption for a typical winter day is 11.33, 11.93 and 9.55 euros for the flat, day/night and dynamic tariffs, respectively. The impact of the tariff structure on the modulation potential is illustrated for one hundred houses for a typical winter day in Fig. 17b. For this example, the modulation parameters are set to $n = 1$, $l = 0$ and $k = 5$. It appears that the flat tariff structure offers the lowest modulation potential. Compared to the day/night tariff, the dynamic structure allows for unlocking of the modulation potential in concentrated time periods, mostly before period 20, between periods 40 and 45 and from period 55 to 65. The dynamic tariff can therefore be tuned to maximize the modulation potential during critical time periods, such as during high imbalance or high day-ahead spot market prices, or to relieve a congestion. The average potential is the highest with the day/night tariff for both upward and downward modulations.

6.7. Illustration with the reserve market

The proposed service can be used to reduce the need for reserve to solve an imbalance at a given time period. However, the resulting cost savings depend on the imbalance tariff, which is unknown at the time of the activation of the modulation. The existence of a rebound effect inherent to TCLs may cause the modulation to become unprofitable. This is illustrated in Fig. 18 for January 24th, 2012, with the corresponding historic imbalance prices. The service parameters are set to $n = 1$, $l = 0$ and $k = 5$. For that specific day, it can be seen that most of the upward modulations performed with this set of one hundred houses are profitable. Most downward activations, contrariwise, are unprofitable. In particular, the activation of a downward modulation

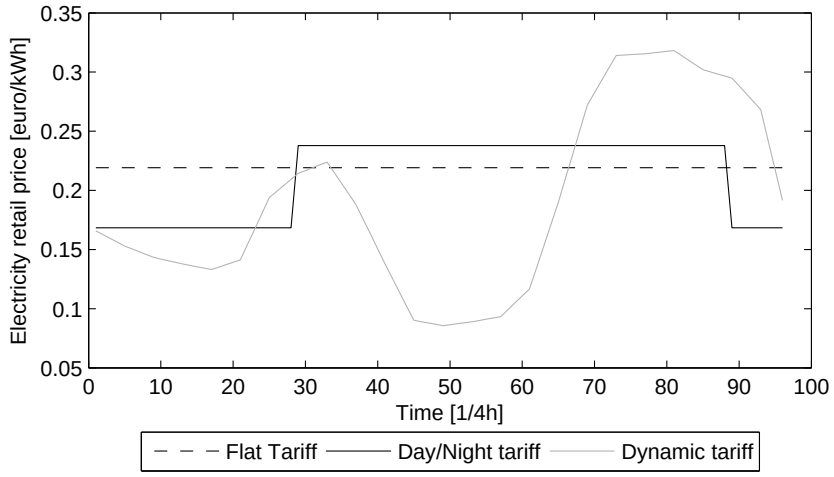

(a) Electricity tariffs.

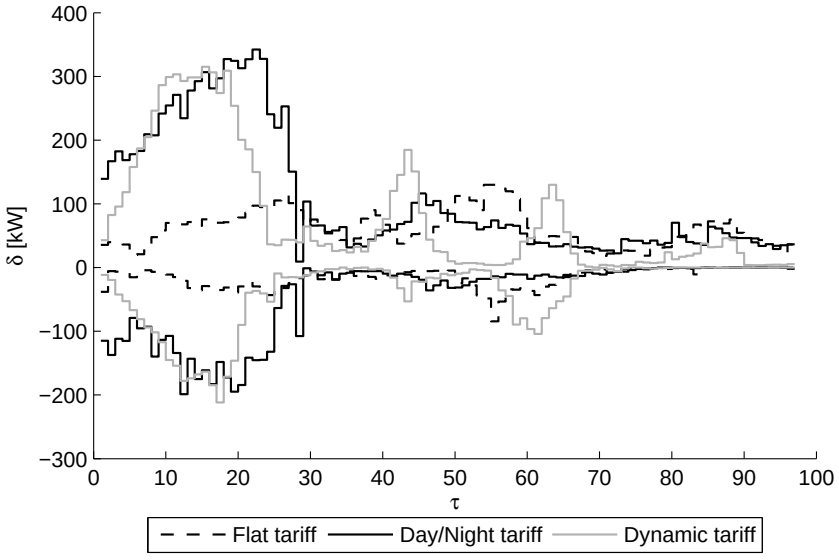

(b) Modulation amplitude.

Figure 17: Impact of the electricity tariff structure on the modulation potential for the aggregated set of 100 houses. Modulation parameters are set to $n = 1$, $l = 0$ and $k = 5$.

when the system imbalance is positive for several consecutive periods leads to an unprofitable activation. This strengthens the conclusion that providing downward modulations with TLCs is more challenging than an equivalent upward modulation. Results may differ as the number of considered houses increases, due to statistical effects of load diversity.

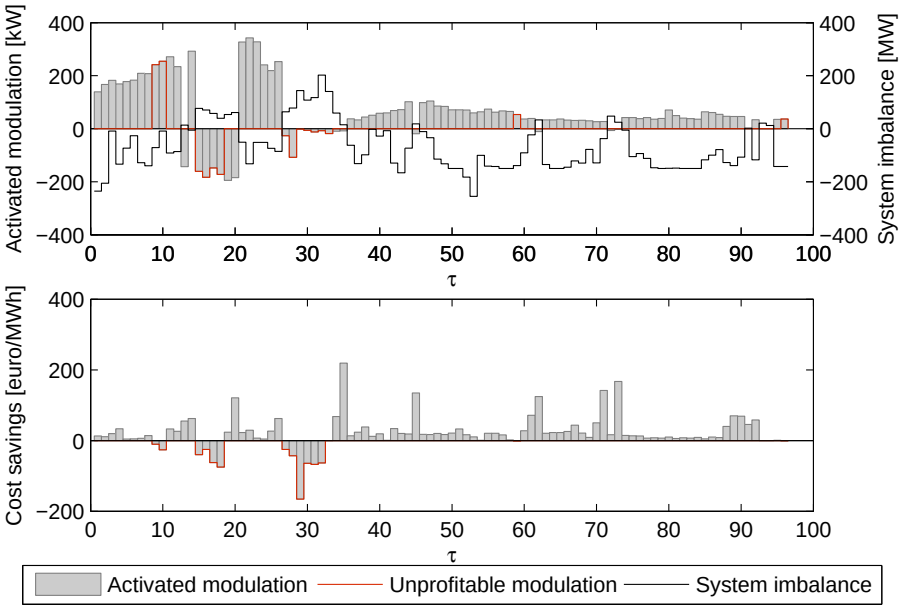

Figure 18: Illustration of the potential cost savings for the activation of the modulation service by an aggregator on the imbalance market on January 24th, 2012. Modulation parameters are set to $n = 1$, $l = 0$ and $k = 5$.

7. Conclusions

This paper presents a flexibility service provided by a load aggregator controlling domestic heat pumps. The heat pumps are used to supply both domestic hot water production and space heating needs. The flexibility service consists of the upward or downward activation of heat pumps at a certain time period and during a given number of periods. The activation is followed by a rebound effect with parametrized deviations from a baseline consumption over a fixed number of periods. This baseline is such that it minimizes the energy costs for the end-user. The rebound effect consists of a delay period with no deviations from the baseline consumption and a payback period during which deviations in consumption occur to allow the heat pumps to

return to their baselines. A sequential optimization scheme is proposed to determine the modulation potential. A variant to the proposed service could be obtained by turning the sequential optimization problem into a combined optimization problem in order to shape the baseline profile so as to obtain the maximum modulation amplitude in a given time period while minimizing the energy costs. The latter is left for future work. The benefits of a desynchronized activation of the heat pumps during the modulation may also be further investigated, as well as and the possibility of additional activations during the rebound effect.

The methodology is first applied to a cluster of houses representative of the Belgian residential building stock. The average modulation potential obtained for a modulation in one time period with no delay and a payback constrained over five periods is 2.9 kW and 0.29 kW per house for an upward modulation and a downward modulation, respectively. Retrofitted or well-insulated freestanding houses enable the most economical modulations, since insulating the building envelope reduces overconsumption. Such houses are then used to further investigate the influence of the parameters characterizing the modulation and rebound effect.

An empirical choice of the weighting parameter between modulation and deviation amplitudes is proposed based on the maximization of the ratio of these amplitudes. Given this choice of weighting parameter, the influence of the time constants of the modulation service is studied. The mean upward and downward modulation amplitudes range from 0.05 to 1.24kW and from 0.01 to 0.5kW, respectively, for paybacks of 15 minutes to one and a half hour. These values decrease by 65% and 72% per house, respectively, for upward and downward modulations for a delay length of thirty minutes, as compared to no delay length. Beyond two periods for the delay length, the average values remain almost unchanged. The limitation in modulation amplitude entailed by increased delay lengths is particularly marked for time periods during the day where the indoor temperature set point is close to a transition. Results show that modulating a group of heat pumps in several consecutive time steps is less efficient than modulating only part of them in each time step. An asynchronous activation of the heat pumps increases the minimum modulation amplitude of the day by 110%. Sensitivity analyses of the modulation potential to the retail tariff structure are also presented. These analyses show that a tuned dynamic retail tariff structure can maximize the modulation potential during critical time periods, for example to relieve a congestion in the network or balancing the electrical system.

The method is applied to the provision of secondary reserve to solve an imbalance for a particular day in the winter. Given the imbalance tariff, results show that, for the given example, all upward modulations are profitable, whereas some downward modulations are not, hereby emphasizing the difficulty to perform downward modulations with TLCs.

Finally, the above results show that with a set of one hundred heat pumps, a load aggregator could expect to harvest mean modulation amplitudes of up to 138kW for an upward modulation and up to 51kW for downward activations, depending on the proposed flexibility service.

References

[1] C. W. Gellings, The concept of demand-side management for electric utilities, Proceedings of the IEEE 73 (10) (1985) 1468–1470.

[2] M. Kamgarpour, C. Ellen, S. E. Z. Soudjani, S. Gerwinn, J. L. Mathieu, N. Mullner, A. Abate, D. S. Callaway, M. Franzle, J. Lygeros, Modeling options for demand side participation of thermostatically controlled loads, in: Bulk Power System Dynamics and Control-IX Optimization, Security and Control of the Emerging Power Grid (IREP), 2013 IREP Symposium, IEEE, 1–15, 2013.

[3] D. Patteeuw, K. Bruninx, A. Arteconi, E. Delarue, W. D'haeseleer, L. Helsen, Integrated modeling of active demand response with electric heating systems coupled to thermal energy storage systems, Applied Energy 151 (2015) 306–319.

[4] R. Halvgaard, N. K. Poulsen, H. Madsen, J. B. Jørgensen, Economic model predictive control for building climate control in a smart grid, in: Innovative Smart Grid Technologies (ISGT), 2012 IEEE PES, IEEE, 1–6, 2012.

[5] K. Hedegaard, O. Balyk, Energy system investment model incorporating heat pumps with thermal storage in buildings and buffer tanks, Energy 63 (2013) 356–365.

[6] R. De Coninck, R. Baetens, D. Saelens, A. Woyte, L. Helsen, Rule-based demand-side management of domestic hot water production with heat pumps in zero energy neighbourhoods, Journal of Building Performance Simulation 7 (4) (2014) 271–288.

[7] M. Miara, D. Günther, Z. L. Leitner, J. Wapler, Simulation of an Air-to-Water Heat Pump System to Evaluate the Impact of Demand-Side-Management Measures on Efficiency and Load-Shifting Potential, Energy Technology 2 (1) (2014) 90–99.

[8] A. J. Conejo, J. M. Morales, L. Baringo, Real-time demand response model, Smart Grid, IEEE Transactions on 1 (3) (2010) 236–242.

[9] G. Masy, E. Georges, C. Verhelst, V. Lemort, P. André, Smart grid energy flexible buildings through the use of heat pumps and building thermal mass as energy storage in the Belgian context, Science and Technology for the Built Environment 21 (6) (2015) 800–811.

[10] R. Renaldi, A. Kiprakis, D. Friedrich, An optimisation framework for thermal energy storage integration in a residential heat pump heating system, Applied Energy, status: in Press .

[11] D. S. Callaway, Tapping the energy storage potential in electric loads to deliver load following and regulation, with application to wind energy, Energy Conversion and Management 50 (5) (2009) 1389–1400.

[12] S. Koch, J. L. Mathieu, D. S. Callaway, Modeling and control of aggregated heterogeneous thermostatically controlled loads for ancillary services, in: Proc. PSCC, 1–7, 2011.

[13] D. Patteeuw, G. Reynders, K. Bruninx, C. Protopapadaki, E. Delarue, W. D'haeseleer, D. Saelens, L. Helsen, CO2-abatement cost of residential heat pumps with active demand response: demand-and supply-side effects, Applied Energy 156 (2015) 490–501.

[14] D. Patteeuw, L. Helsen, Residential buildings with heat pumps, a verified bottom-up model for demand side management studies, in: Proceedings of 9th International Conference on System Simulation in Buildings (SSB), 2014.

[15] D. Wang, S. Parkinson, W. Miao, H. Jia, C. Crawford, N. Djilali, Online voltage security assessment considering comfort-constrained demand response control of distributed heat pump systems, Applied Energy 96 (2012) 104–114.

[16] S. Mathieu, D. Ernst, Q. Louveaux, An efficient algorithm for the provision of a day-ahead modulation service by a load aggregator, in: Innovative Smart Grid Technologies Europe (ISGT EUROPE), 2013 4th IEEE/PES, IEEE, 2013.

[17] S. Mathieu, Q. Louveaux, D. Ernst, B. Cornélusse, A quantitative analysis of the effect of flexible loads on reserve markets, in: Proceedings of the 18th Power Systems Computation Conference (PSCC), IEEE, 2014.

[18] G. S. Pavlak, G. P. Henze, V. J. Cushing, Optimizing commercial building participation in energy and ancillary service markets, Energy and Buildings 81 (2014) 115–126.

[19] G. S. Pavlak, G. P. Henze, V. J. Cushing, Evaluating synergistic effect of optimally controlling commercial building thermal mass portfolios, Energy 84 (2015) 161–176.

[20] R. De Coninck, L. Helsen, Quantification of flexibility in buildings by cost curves–Methodology and application, Applied Energy 162 (2016) 653–665.

[21] M. Ali, A. Alahäivälä, F. Malik, M. Humayun, A. Safdarian, M. Lehtonen, A market-oriented hierarchical framework for residential demand response, International Journal of Electrical Power & Energy Systems 69 (2015) 257–263.

[22] M. Goldberg, Measure twice, cut once, Power and Energy Magazine, IEEE 8 (3) (2010) 46–54.

[23] D. F., F. Ollivier, A. Poblador, Grey boxes used to represent buildings with a minimum number of geometric and thermal parameters, Energy and Buildings 31 (1) (2000) 29 – 35.

[24] International Standard Organization, ISO13790:2007 : . Energy performance of buildings – Calculation of energy use for space heating and cooling, Geneva, Switzerland, 2007.

[25] A. Bolher, R. Casari, E. Fleury, D. Marchio, M. J., Méthode de calcul des consommations d'énergie des bâtiments climatisés ConsoClim, Tech. Rep., Ecole des Mines (Paris), 1999.

[26] S. Gendebien, E. Georges, S. Bertagnolio, V. Lemort, Methodology to characterize a residential building stock using a bottom-up approach: a case study applied to Belgium, International Journal of Sustainable Energy Planning and Management 4 (2015) 71–88.

[27] Bureau of standardization, EN14511 - 2 (2008) : Air conditioners, liquid chilling packages and heat pumps with electrically driven compressors for space heating and cooling - Part 2: test conditions, European Standard, 2007.

[28] E. Georges, S. Gendebien, S. Bertagnolio, V. Lemort, Modeling and simulation of the domestic energy use in Belgium following a bottom-up approach, in: CLIMA 2013 11th REHVA World Congress & 8th International Conference on IAQVEC, 2013.

[29] J. Lofberg, YALMIP: A toolbox for modeling and optimization in MATLAB, in: Computer Aided Control Systems Design, 2004 IEEE International Symposium on, IEEE, 284–289, 2004.

[30] I. ILOG, CPLEX Optimization Studio, 2013.

[31] American Society of Heating, Refrigerating and Air-Conditioning Engineers (ASHRAE, ASHRAE standard 55 :Thermal Environmental Conditions for Human Occupancy, 1992.

[32] Elia, Imbalance prices, URL http://www.elia.be/en/grid-data/balancing/imbalance-prices, 2012.

[33] E. Parliament, 2010 Energy Performance of Buildings Directive, 2010.

Nomenclature

This section defines the main symbols used in this paper. Others are defined as required in the text.

Parameters

H	Number of periods in the horizon
$\mathcal{H}$	Optimization horizon $\{1, \ldots, H\}$
n	Number of modulation periods
l	Number of delay periods before payback
k	Number of payback periods
$\mathcal{K}(\tau, (n-1)+l+k)$	Flexibility service horizon $\{\tau, \tau+1, \ldots, \tau+(n-1)+l+k\}$
$\mathbf{A}^i$, $\mathbf{B}^i$, $\mathbf{E}^i$	Parameters of state-space model
C	Thermal capacitance
c_i, d_i, f_i	Parameters of the heat pump model
dt	Period duration
COP_t	Heat pump coefficient of performance
ϵ	Penalty for the payback imbalance
Γ_t	Exogenous power consumed
Q_t^g, Q_t^{sol}	Internal heat gains, solar gains
π_t^+	Buying price of electricity
π_t^-	Selling price of electricity
R	Thermal resistance
σ	State deviation tolerance from baseline
λ	State constraint relaxation
T_t^a	Ambient temperature
T_t^{su}	Water supply temperature
$\mathbf{u}_t$	State-space model parameters
$\mathbf{x}^i$	Initial state

Variables

δ_t	Modulation amplitude
δ_τ^*	Minimum modulation amplitude over n periods
I^+	Maximum positive deviation after a modulation
I^-	Maximum negative deviation after a modulation
P_t	Total consumption
P_t^+	Power bought from the grid
P_t^-	Power sold to the grid
Q_t	Heat pump thermal capacity
T_t	Temperature
W_t	Compressor electrical power consumption
$\mathbf{x}_t$	State variable
y_t	Heating mode

Powers are taken as positive when consumed and negative when produced. A positive modulation corresponds to an increase in consumption. Variables obtained for the baseline are denoted with a $\hat{\bullet}$.

Superscripts

g	gain
sol	solar
n	nominal
a	ambient
w	water
su	supply
s	space heating
i	indoor
m	massive
l	light
int	internal

Acknowledgment

F.R.S-FNRS in Belgium is gratefully thanked for funding Research Fellow Emeline Georges.